WOOD PROPERTIES OF FOUR TROPICAL SPECIES FROM MINING AREAS IN AMAZON, BRAZIL, PART 1: ANATOMICAL CHARACTERIZATION

*J. L. L. Abreu**
Graduate Student
E-mail: juliana.lima.abreu@gmail.com

M. G. Silva
Assistant Professor
E-mail: marcela.gsilva@gmail.com

G. C. Ferreira
Professor and Department Head
Department of Forest Science
Federal Rural University of Amazonia
66077-830 Belem, Brazil
E-mail: gracialdaf@yahoo.com.br

T. S. F. A. França†*
Assistant Professor
Department of Sustainable Bioproducts
Mississippi State University
Mississippi State, MS 39762-9820
E-mail: tsf97@msstate.edu

A. R. C. Reis
Professor and Department Head
Department of Forest Science
Federal University of Pará
68372-040 Belem, Brazil
E-mail: alissonreis@ufpa.br

V. M. S. Pamplona
Professor and Department Head
Department of Forestry Engineering
Federal University of Pará
68627-451 Paragominas, Brazil
E-mail: alissonreis@ufpa.br

(Received October 2022)

Abstract. Mining is an essential economic activity in Brazil, but it causes several negative impacts, including deforestation. Vegetation suppression is a common activity in mining areas, and it generates large volumes of discharged logs from excavation activity. In most cases, these logs are stacked and stored in open-air yards, as a result, the material is exposed to conditions that favor the degradation process. To minimize these impacts, the goal of this research was to anatomically characterize and determine some of the physical properties of wood species that are species wasted in open mining areas and to evaluate their potential uses. Due to the lack of anatomical information of the species studied, the objective of Part 1 of

* Corresponding author
† SWST member

this study was to characterize the anatomical features of tropical species stored in bauxite mining areas located in the Amazon rainforest. Wood samples were identified and collected in Paragominas (Pará), Brazil, during five different exposure periods (0, 1, 4, 6, and 8 yr of exposure). The species identified and studied were *Jacaranda copaia*, *Astronium lecointei*, *Caryocar villosum*, and *Protium altissimum*. Three logs were collected from each species and each year of exposure, totaling 54 specimens used for the anatomical analysis of the microstructure of the species studied. Anatomical structures were characterized, and degradation signs were also observed in some species, where *Jacaranda copaia*, a lower-density species, showed higher levels of degradation.

Keywords: Wood anatomy, wood characterization, Amazon forest, tropical species.

INTRODUCTION

The state of Pará is in northern Brazil and is traversed by the lower Amazon River where the main economic activities include wood products, mining, and agriculture (Kuresk et al 2020). In the mid-70 s, governmental incentives were given by the government, and many industries were encouraged to populate the Amazon region, which attracted new industries such as mining, wood industries, and agricultural companies to the region (Mahar 1988).

According to Parrotta and Knowles (2002), it is estimated an annual loss of 2000-3000 ha of tropical forest in Brazil due to opencast mining for bauxite, cassiterite, iron, manganese, and kaolin has resulted.

Vegetation suppression is one of the several negative impacts the mining activities, resulting in a significant amount of waste of natural resources (Ripley and Redmann 1996; Dudka and Adriano 1997). Large volumes of natural resources and old-growth forests are extracted and moved during mining activities. As the demand for minerals continues to rise, a significant impact on the ecosystem and biodiversity present in the forest will continue (Silva et al 2012).

A portion of the extracted volume is the wood coming from the vegetation suppression area. This material, once removed from the ground, is stored in open-air storage yards in the project's areas until its destination. However, when the wood is left for a long time and the right conditions are given to biotic agents, the deterioration process starts to occur, mainly driven by fungi (Sgai 2000; Arantes and Milagres 2009).

In Eastern Amazon, more specifically in the state Pará, open-pit mining operations of iron ore and bauxite are a common activity, resulting in a large waste of natural products that are left behind in open areas, under conditions that will facilitate the degradation of wood, and used for the material that is wasted should be evaluated, and a need has emerged to understand the material and identify potential uses for these resources.

Species found in mining areas have commercial relevance and if the condition of the material is well understood, these resources will be able to be used.

One of the main knowledge areas needed to better use wood as a material is the understanding of anatomical structure. These types of studies are important to understand the role environmental factors play in the anatomical and physical properties of the wood material (Burger and Richter 1991; Gomes et al 2002).

In addition, anatomical observations can be used to identify signs of successive stages of decay in wood over time. Since a number of fungi cause modifications in the wood cells, the analysis of anatomical structure can end-users decide if the material can be still used even after long-term exposure to degradation conditions (Wilcox 1968, 1970; Zabel and Morell 2020). Anagnost (1998) cites that boreholes, the shape of erosion channels, and cavities are some features that can be used to decay in wood, which can limit the uses of the material.

Soares et al (2013) state that basic knowledge of anatomical features of wood species native to the

Amazon rainforest is crucial for this material to be properly explored. One of the key factors for the inadequate use of Amazonian species is the lack of misidentification of commercialized species, which compromises the final use of this raw material.

Because the wood products industry is an economic activity in the Amazon and limited information on the species presented in this study, the objective of this study was to evaluate the properties of four tropical wood species exposed in different periods in a bauxite-mined site located in Paragominas (Pará), Brazil. Part 1 of this research focused on the anatomical identification and characterization of these species, which provides a better understanding of the degradation stage of these species.

MATERIALS AND METHODS

Samples Preparation

Logs analyzed in this study were collected from open-air storage yards and originated from plant suppression for bauxite exploration in the municipality of Paragominas, Pará, Brazil. The suppressed woods were stored in accordance with the Plant Suppression Authorization and distributed in the areas of the Miltônia III plateau (Fig 1).

The climate in this locality is classified as Aw, and the average temperature is 26.5°C. The months from June to November represent the driest season, with a minimum precipitation of 17 mm and a maximum of 62 mm, with RH between 62% and 81%, while between December and May, precipitations between 119 and 380 mm are registered, with RH reaching up to 89%.

The area of this study was located in the municipality of Paragominas (southeast of Pará), where bauxite extraction is practiced, by the strip mining method, open-pit mining in strips longitudinal, which consists of removing the first layer of soil (considered sterile material), followed by excavation to remove the ore. At the end of this process, the sterile material remains in the mining area, in a place adjacent to the excavation (Pimentel 2009; Cerqueira et al 2021).

Four species were selected: *Jacaranda copaia* (Aubl.) D.Don, *Astronium lecointei* Ducke, *Caryocar villosum* (Aubl.) Pers., and *Protium altissimum* (Aubl.). These species were chosen because they were the most frequent species found in the area studied (Fig 2). Because of the similarity of species, a series of identification steps were conducted in the field and at the laboratory. In the field, the identification of species was carried out based on dendrological features followed by macroscopic identification of logs in the laboratory. Once species were confirmed, disks from the ends of species were removed.

From each species, three replicates (logs) of different piles were collected from five storage periods: 8, 6, 4, 2, and <1 yr – considered year 0. Because of the advanced stage of deterioration of *Jacaranda copaia*, it was not possible to collect samples for years 6 and 8. Then a total of nine disks were collected for *Jacaranda copaia*, and 15 disks were collected for *Astronium lecointei*, *Caryocar villosum*, and *Protium altissimum*, totaling 54 samples.

The material was then moved to the laboratory and cleaned using a brush to remove any debris from the field. Another set of wood identification tests was conducted to ensure that the species collected were correctly identified. The disks were oven-dried at 60°C for 48 h to reduce MC. From each disc collected, three specimens were removed from the heartwood portion, with an approximate size of 2 cm × 2 cm × 2 cm (transverse × tangential × radial). The overall summary of species and anatomical features analyzed in this study is shown in Table 1.

Anatomical Characterization

Macroscopic features. Once the species were confirmed three specimens were removed from the heartwood portion of each disc collected, with an approximate size of 2 cm × 2 cm × 2 cm (transverse × tangential × radial). The macroscopic characterization was performed using a sharp disposable blade, in which the anatomical planes were flattened for better visualization of the anatomical structures, and a 10× magnifying

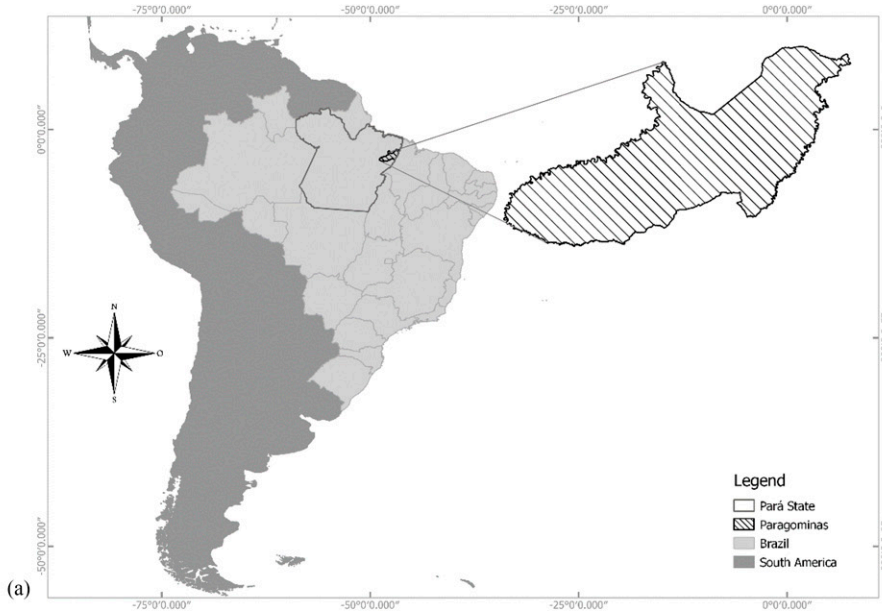

(a)

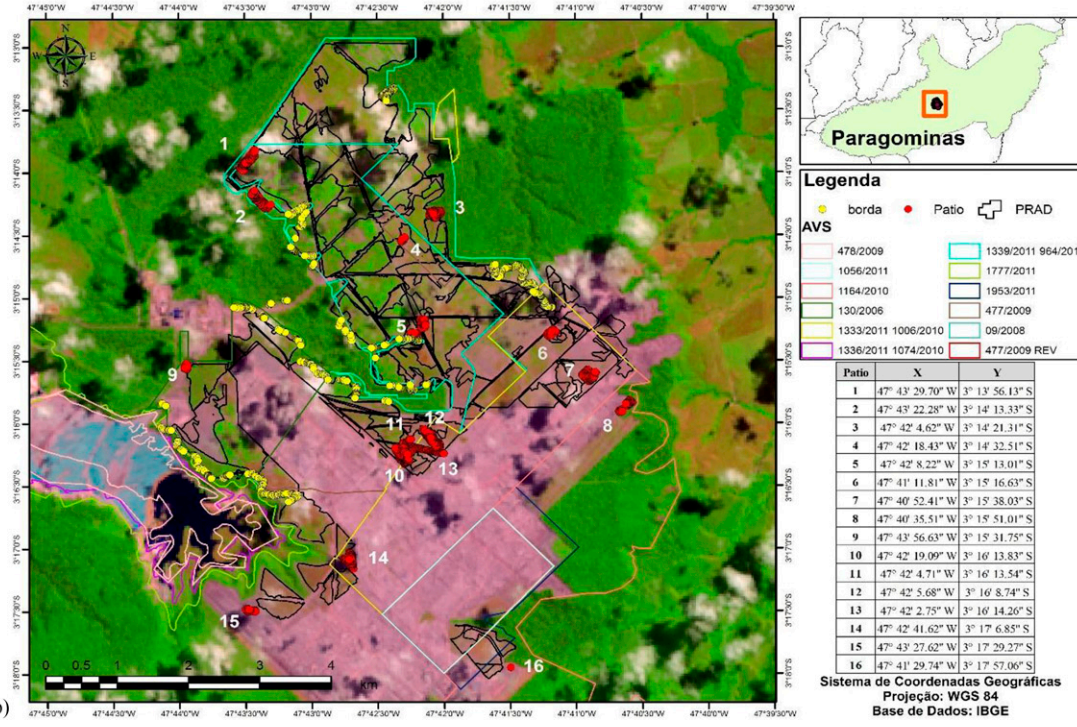

Patio	X	Y
1	47° 43' 29.70" W	3° 13' 56.13" S
2	47° 43' 22.28" W	3° 14' 13.33" S
3	47° 42' 4.62" W	3° 14' 21.31" S
4	47° 42' 18.43" W	3° 14' 32.51" S
5	47° 42' 8.22" W	3° 15' 13.01" S
6	47° 41' 11.81" W	3° 15' 16.63" S
7	47° 40' 52.41" W	3° 15' 38.03" S
8	47° 40' 35.51" W	3° 15' 51.01" S
9	47° 43' 56.63" W	3° 15' 31.75" S
10	47° 42' 19.09" W	3° 16' 13.83" S
11	47° 42' 4.71" W	3° 16' 13.54" S
12	47° 42' 5.68" W	3° 16' 8.74" S
13	47° 42' 2.75" W	3° 16' 14.26" S
14	47° 42' 41.62" W	3° 17' 6.85" S
15	47° 43' 27.62" W	3° 17' 29.27" S
16	47° 41' 29.74" W	3° 17' 57.06" S

Sistema de Coordenadas Geográficas
Projeção: WGS 84
Base de Dados: IBGE

(b)

Figure 1. Location of mining area. (a) Geographical location of mining. (b) Distribution map of logs storage in of the Miltônia III plateau.

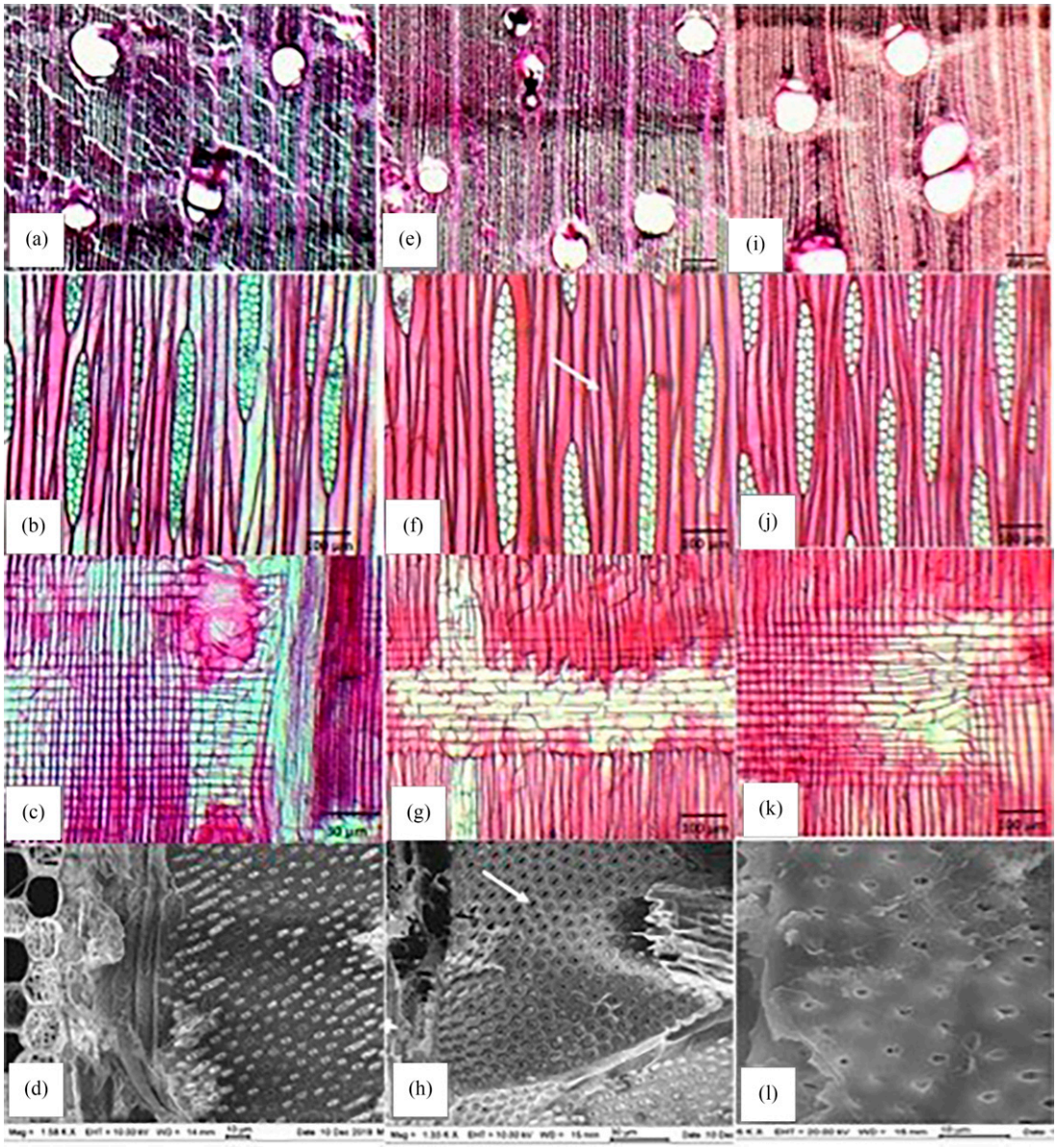

Figure 2. Anatomical elements of *Jacaranda copaia* from microscopic analysis. The arrows on the pictures indicate the following: (a-d) Wood with 4 yr of storage, (e-h) with 2 yr of storage, and (i-m) with a period of less than 1 yr of storage. Scale bars: (a, e, and i) 200 µm; (b, f, j, g, and l) 100 µm; (h) 30 µm; and (d and m) 10 µm.

glass was used. The organoleptic properties such as smell and taste were not taken into account because it is material from storage, which in turn has gradually lost these characteristics according to the storage time.

Coradin and Muñiz (1992) procedures were followed for the macroscopic characterization traditional method for tropical timber classification. In addition, photomacrographs were taken at the Laboratory of Plant Taxonomy of the Museu

Table 1. Overall information of each species and anatomical features studied.

Scientific name	Common name	Vessel	Rays	Fibers
Jacaranda copaia (Aubl.) D. Don	Parápará	Frequency (mm^{-2})	Length (μm)	Length (μm)
Astronium lecointei Ducke	Muiracatiara	Vessel grouping (%)	Width (μm)	Wall thickness (μm)
Caryocar villosum (Aubl.) Pers.	Piquiá	Vessel arrangement	Height (cell counts)	Lumen thickness (μm)
Protium altissimum (Aubl.)	Breu Barrote	Length (μm)	Width (cell counts)	—
		Width (μm)	Frequency (mm^{-1})	—

Paraense Emílio Goeldi (LABTAX-MPEG) using an optical Stereomicroscope – Zeiss, model: Discovery was used. V8 coupled to an AxioCam ICc 5 camera, with a photographic resolution of 2452 × 2056 and Zen 2.3 lite software. Validation of wood identification was also performed at Museu Paraense Emílio Goeldi Zeiss, Oberkochen, Germany.

Microscopic feature – macerate and histological sections. To obtain the macerated material, longitudinal fragments were removed from each specimen and inserted into penicillin flasks with 8 mL of the macerating solution, using the Franklin method (1945), a solution consisting of glacial acetic acid and hydrogen peroxide in the proportion of 1:1, and kept in an oven at 60°C for 24 h until the material was completely bleached. Then, the macerating solution was removed, and later the dissociated material was washed in distilled water four times, using the decantation process.

The material was then stained with 1% aqueous safranin and preserved in distilled water. To observe the dissociated cellular elements, an average of 40 temporary slides were made of each sample by mixing a small amount of the macerated material in drops of glycerin.

For the histological sections, the specimens were submerged in distilled water for 24-72 h for softening and trimming, and the most resistant material was boiled in 1:4 water and glycerin solution for 7-10 h. Using a Reich slide microtome, histological sections were obtained in the three anatomical planes with thicknesses varying from 18 to 25 μm. These were divided into two groups, one of them was submitted for clarification and coloring and the other was kept in the wild for the observation of possible mineral inclusions. For tissue staining, the Johansen (1940) technique was used.

Part of the material preserved in its natural state went through the dehydration process in a progressive ethanol series (60%, 70%, 80%, 90%, and absolute alcohol) lasting 60 min each ethanol series and then stored in a container with silica gel and subjected to scanning electron microscopy (SEM) and energy dispersion X-ray spectroscopy (EDS), at the Microanalysis Laboratory of the Geology Institute of the Federal University of Pará.

Measurement of anatomical elements. A digital analysis system in Motic Image plus 3.0 Software with MOTIC BA310-E microscope was used for the measurements, and a total of 50 replicates per parameter was collected. All anatomical characterization, measurement techniques, and terminology followed the IAWA Committee (1989) procedures. All images were analyzed using Motic Image plus 3.0 Software, Motic Asia, Kowloon, Hong Kong.

Energy dispersive spectroscopy. If the presence of crystals was noted during the microscopic analysis, EDS analyses were performed to determine the chemical components present in the samples. EDS analyses were performed at the Microanalysis Laboratory of the Geosciences Institute at the Federal University of Para. The equipment used was a Zeiss SEM model LEO-1430 with EDS IXRF model Sirius-SD coupled. The operating conditions were electron beam current = 90 μA, constant acceleration voltage = 20 kV, working distance = 15 mm, and counting time for element analysis = 30 s.

Statistical Analysis

Descriptive analysis was performed using mean, standard deviation, and coefficient of variation. The parameters were analyzed following a completely randomized design. Statistical analysis was performed using the AgroEstat, Barbosa and Maldonado (2015), and IBM SPSS programs, Chicago, IL, USA.

To verify the assumptions for the application of the analysis of variance, the data were submitted to the Levene homogeneity of variances and Kolmogorov-Smirnov normality tests, while the independence of the residuals was performed by means of graphical analysis. When the assumptions were not met, the Box-Cox transformation was applied to the data, and these transformed data were used to perform the statistical analysis. However, to facilitate the understanding of the results, they were presented with untransformed data.

To analyze whether there was a significant difference between species and storage exposure, an F test was performed, and when differences were observed, the Tukey test was performed at 5% of significance. To analyze the trend in the behavior of anatomical variables as a function of storage time, adjustments were made to linear and quadratic polynomial regression models for each species. These models were chosen because of their wide adaptation to describe biological phenomena.

The selection of the most adequate model to explain the behavior of each parameter evaluated was carried out using the following criteria: 1) significance of the regression model using the F test, 2) coefficient of determination, and 3) residual standard deviation.

RESULTS AND DISCUSSION

General Overview of Each Species

Jacaranda copaia belongs to the Bignoniaceae family, and it is a widely occurring species in the states that make up the Amazon biome, located in the northern region of Brazil (Farias-Singer 2020). It can reach up to 35 m in height and 0.7 m in diameter. The wood has commercial relevance and is often obtained from sustainable forest management projects in the region. In addition, it is often used in the recovery of areas degraded by agriculture in the Central Amazon and promotes a positive response to the chemical attributes of the soil (Santos and Miller 1997; Barbosa et al 2003; Machado et al 2017; Ferreira et al 2021).

Protium altissimum, Burseraceae family, is commonly found in all states of the northern region of Brazil being considered a hyperdominant species, and it is the second most abundant species in the Amazon. The trees can reach up to 30 m in height, with wood of great economic value, and can also be used as medicine and food (Gomes et al 2019; Piva et al 2020; Ferreira et al 2021; Spletozer et al 2023).

Caryocar villosum from the Caryocaraceae family, is known in the Amazon as Piquiá. Trees from this species are distributed in the central and eastern Amazon and are considered giants of nature, reaching more than 40 m in height and up to 2 m in diameter. It is very durable over time and commonly used in the manufacturing of boats in the Amazon region because of its good resistance to attack by xylophagous organisms. Piquiá is considered highly resistant in field trials in the Cerrado biome and resistant to hemiparasites in urban afforestation in the Amazon (Braga Júnior et al 2020; Braga et al 2021; Silveira et al 2021; Albuês et al 2023; Prance and Pirani 2023).

Astronium lecointei belongs to the Anacardiaceae family, and trees of this species occur frequently in the northern states of Brazil. Trees can reach an average of 25 m in height and can have diameters of up to 0.6 m. It is considered a highly resistant species in field trials in the Amazon biome, with a lifespan of 27 yr, and the wood has high density (0.94 g cm^{-3}) and easy workability (Silveira et al 2021; Silva-Luz et al 2023).

Anatomical Features

A summary of the anatomical features of *Jacaranda copaia* is presented in Table 2. Figure 2 shows the general macroscopic view of samples in each year of exposure. The data for *Jacaranda*

Table 2. Anatomical characters of *Jacaranda copaia* in different storage time (yr).

Anatomical features		Years of exposure			Overall mean
		4	2	0	
Fibers	Length (μm)	1249.94	1211.28	988.30	1157.36
	Wall thickness (μm)	2.72	2.62	2.27	2.55
	Lumen thickness (μm)	20.68	22.48	19.05	20.81
Vessels	Length (μm)	476.43	481.04	405.24	456.51
	Diameter (μm)	213.09	256.26	221.44	230.67
Rays	Height (μm)	328.60	305.47	364.44	331.37
	Width (μm)	32.70	34.17	33.40	33.42
	Height (cell counts)	15.70	14.53	15.80	15.32
	Width (cell counts)	2.03	2.46	2.34	2.27
	Frequency (mm^{-1})	4.39	4.58	5.06	4.66

copaia were collected only in years 0, 2, and 4 due to the advanced stage of deterioration. Figure 3 shows the anatomical features in macerate analysis and microscopic views of *Jacaranda copaia*.

In samples with 4 yr of exposure, cracks in the fiber lumen (Fig 3[a]) and in the vessel elements were observed. Fibers with end split were present (Fig 3[b]-[d]). Distinct growth layers were individualized by darker transverse fibrous zones (Fig 1[e]). Pores/vessels were visible to the naked eye, diffuse, with an arrangement tending to the diagonal, with an average length of 466 μm and an average width of 230 μm, with 73% solitary, 23% multiples of 2, 3% multiples of 3, and 1% multiples of >4, with angular contour, simple perforation plate (Fig 3[f]). Pits were occurring

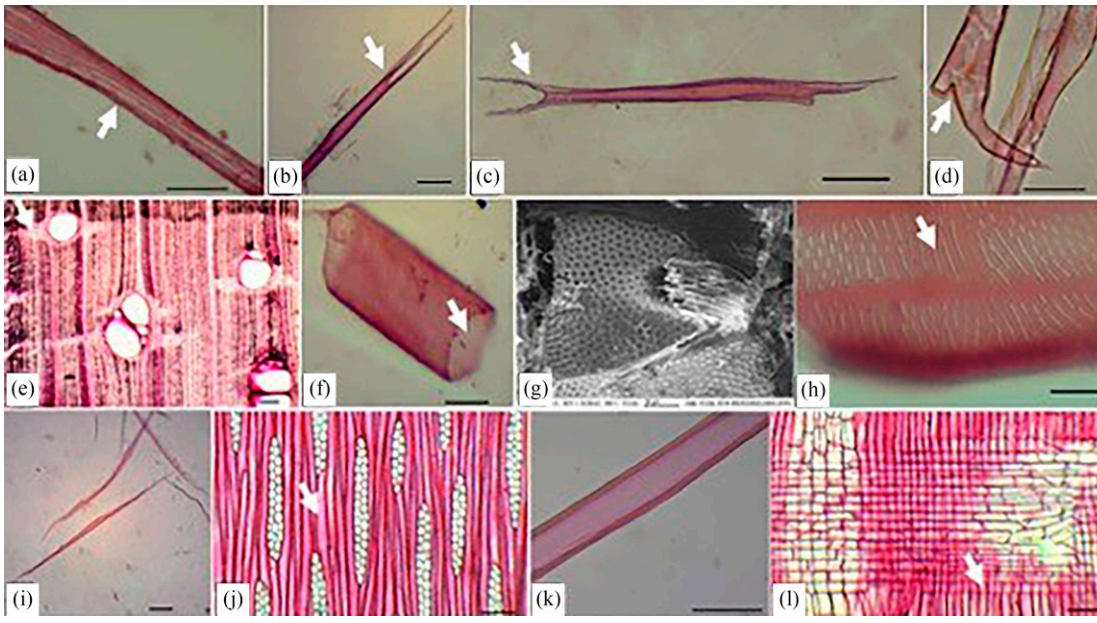

Figure 3. Anatomical features observed in *Jacaranda copaia*. The arrows on the pictures indicate the following: (a) indicates cracks in the lumen, (b-d) bifurcated fibers in macerated material, (e) growth layers, (f) simple perforation plate, (g) alternate pits in vessels from scanning electron microscope, (h) scalariform pits, (i-l) nonseptate fibres, and (m) rays with square and/or erect cells on the radial plan. Scale bars: (a, d, h, and L) 50 μm; (b, c, f, j, and m) 100 μm; and (e and i) 150 μm.

scalariform (Fig 3[g]) and alternating (Fig 3[h]). Libriform fibers (Fig 3[i]) and nonseptate fibers (Fig 3[j] and [l]), with a mean length of 1157.35 μm. Axial parenchyma visible to the naked eye, paratracheal aliform with a linear extension being elongated and narrow (also shown in Fig 3[e]), occasionally occurs confluent with five to eight cells per strand of parenchyma.

Rays visible to the naked eye in transverse and tangential sections, not stratified, with an average height of 331 μm and an average width of 33 μm, consist of a body of procumbent cells mainly with two to four rows of square and/or erect (Fig 3[m]). Marginal cells in macroscopic observation mirroring of the spokes were considered contrasted in the radial section. Ray-vascular pits with distinct borders, similar to intervessels in size and shape, and mirrored rays in macroscopic observation when contrasted in the radial section.

The anatomical characterization found in this study is similar to the ones reported by Paula (1977), Santos and Miller (1997), and Pace et al (2015). Characteristics such as paratracheal aliform with linear extension, distinct growth layers, and nonstratified rays were also observed by Costa (2017), who used the impulse excitation technique to classify Amazonian woods for string instrument composition purposes. Also, the results of this study were similar to that of Rodrigues (2023), who evaluated glued laminated structural elements made with *Jacaranda copaia* wood, and that of Cahuana et al (2021), who analyzed the dendrochronology of *Jacaranda copaia* influenced by the El Niño phenomenon, which occurs in Peru.

Figure 4 shows microscopic and macerate analysis in *Astronium lecointei*, and Table 3 shows the summary of the anatomical features. Distinct growth layers were individualized by darker transverse fibrous zones (Fig 5[a]). Pores/vessels are visible only under a 10× magnification lens and are diffused with an arrangement without a defined pattern, sometimes tending to the diagonal, with an average length of 338 μm and an average width of 134 μm, 60% solitary, 19% multiples of 2.10% multiples of 3 and 5% multiples of 4 and 6% multiples of >4, sometimes obstructed by shiny or whitish substance macroscopically and by tylosis microscopically (Fig 5[b]) with simple perforation plate, circular contour, under observation macroscopically; the vascular lines were straight in the tangential section, alternating intervessel pits, vascular ray pits with very reduced borders to apparently simple. Libriform and septate fibers (Fig 5[c] and [d]), with an average length of 1139 μm. Axial parenchyma was visible only under a 10× magnification lens, scarce paratracheal, and a vasicentric type in lesser quantity. The presence of crystals in parenchyma cells was observed (Fig 5[e]). Rays were visible to the naked eye in transverse and tangential sections, nonstratified, with an average height of 345 μm and an average width of 23 μm, consisting of a procumbent cell body, mainly with 2-4 rows of marginal cells, and the presence of fused rays (Fig 5[b]), sometimes with the content composed of carbon, was verified in EDS analysis (shown previously in Fig 5[d]). In macroscopic observation, the mirror of the rays was considered contrasted in the radial section. Prismatic crystals of calcium oxalate were observed in square ray cells (Fig 5[f] and 5[g]).

Distinct growth layers, scanty parenchyma, and prismatic crystals were observed by Gonçalves and Scheel-Ybert (2016) and Duarte et al (2021), and the presence of tylosis was observed by Melo et al (2013).

For *Caryocar villosum*, the anatomical and macerate analyses are shown in Fig 6 and the summary for the anatomical feature is shown in Table 4. Different growth layers are individualized either by a layer of fibrous tissue (Fig 7[a]) or by bands of parenchyma simulating marginal parenchyma (Fig 7[g]). Pores/vessels were visible only under a 10× magnification lens; diffuse, radial arrangement, with an average length of 570 μm and an average width of 215 μm, 58% solitary, 28% multiples of 2, 9% multiples of 3, 2% multiples of 4, and 2% multiples of >4, obstructed by a shiny substance macroscopically and by tylosis microscopically (Fig 7[b]), with a simple perforation plate, circular contour. In macroscopic observation, the vascular lines were

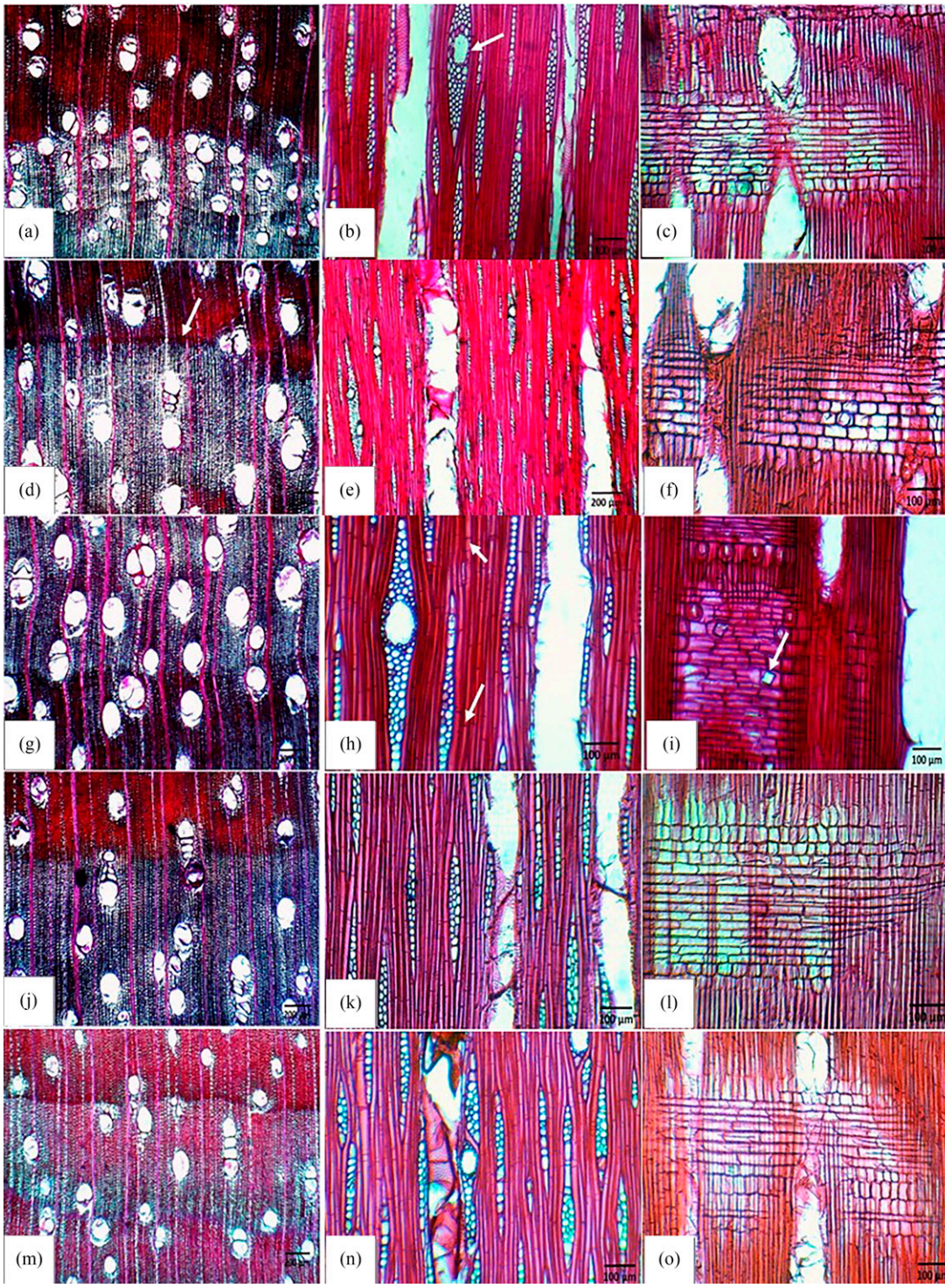

Figure 4. Anatomical elements of *Astronium lecointei*. The arrows on the pictures indicate the following: (a-c) With 8 yr of storage, (d-f) with 6 yr of storage, (g-i) with 4 yr of storage, (j-m) with 2 yr of storage, and (n-p) with a period of less than 1 yr of storage. Scale bars: (a, d, e, g, j, and n) 200 µm and (b, c, f, h, i, l, m, o, and p) 100 µm.

Table 3. Anatomical characters of *Astronium lecointei* in different storage time (yr).

Anatomical features		Years of exposure					Overall mean
		8	6	4	2	0	
Fibers	Length (μm)	1138.02	1169.55	1331.43	1225.66	833.50	1139.63
	Wall thickness (μm)	4.14	4.87	5.18	5.02	3.45	4.53
	Lumen thickness (μm)	8.38	6.90	6.36	7.46	4.42	6.70
Vessels	Length (μm)	352.39	343.46	327.45	342.12	327.53	338.59
	Diameter (μm)	131.73	131.52	138.39	152.76	117.36	134.35
Rays	Height (μm)	324.01	362.09	363.84	342.71	334.81	345.52
	Width (μm)	27.22	24.27	19.40	23.77	22.88	23.51
	Height (cell counts)	15.33	16.14	15.57	16.75	17.31	16.22
	Width (cell counts)	2.55	2.01	1.47	2.37	1.85	2.05
	Frequency (mm^{-1})	6.25	6.81	6.43	6.01	7.10	6.52

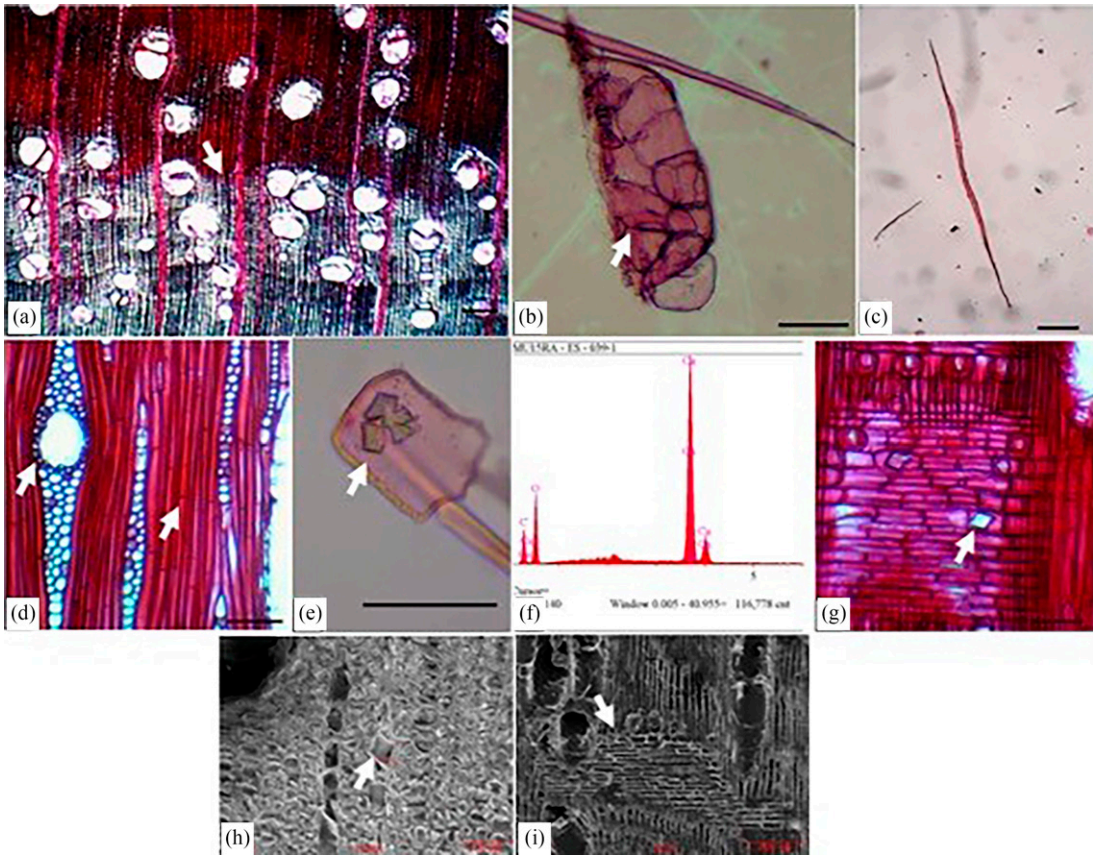

Figure 5. Anatomical features observed *Astronium lecointei*. The arrows on the pictures indicate the following: (a) growth layers, (b) tylosis in vessels from macerate material, (c) libriform fibers, (d) fusiform ray and septate fiber, (e) prismatic crystals in chambered parenchyma cells, (f) energy dispersion X-ray spectroscopy confirming the presence of calcium, and (g-i) prismatic crystals in chambered ray cells.

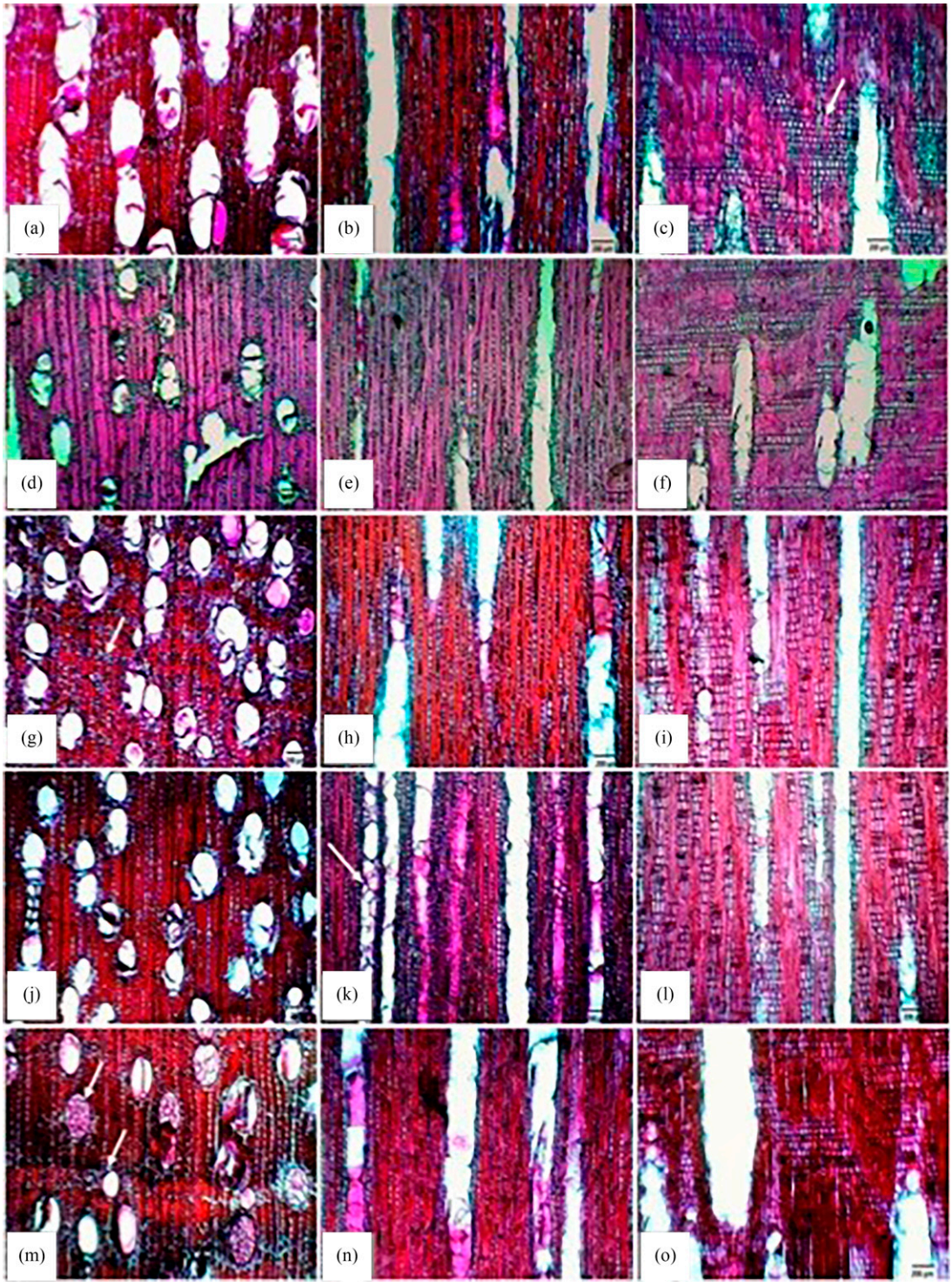

Figure 6. Anatomical elements observed in macerated material from *Caryocar villosum*. The arrows on the pictures indicate the following: (a, c, e, f, and h) With 8 yr of storage and (b, d, g, i, and j) with a period of less than 1 yr of storage. Scale bars: (a-p) 200 μm.

Table 4. Anatomical characters of *Caryocar villosum* in different storage time (yr).

Anatomical features		Years of exposure					Overall mean
		8	6	4	2	0	
Fibers	Length (μm)	2256.18	2146.81	2303.59	2485.98	2353.52	2309.22
	Wall thickness (μm)	8.43	8.73	8.01	9.15	9.48	8.76
	Lumen thickness (μm)	3.25	2.36	2.95	2.08	2.02	2.53
Vessels	Length (μm)	566.01	512.16	592.76	572.48	606.62	570.01
	Diameter (μm)	190.86	192.68	220.83	228.86	243.62	215.37
Rays	Height (μm)	623.46	559.80	631.72	771.33	785.66	674.39
	Width (μm)	18.22	26.97	18.15	21.04	18.92	20.66
	Height (cell counts)	26.96	21.42	24.06	27.49	25.55	25.09
	Width (cell counts)	1.79	1.70	1.68	1.55	1.61	1.67
	Frequency (mm^{-1})	10.91	11.17	11.35	10.72	9.96	10.82

straight in section tangential, alternating intervessel pits and scalariform, horizontal ray vascular pits (scalariforms, gash-like) (Fig 7[c]). Nonseptate fibers were, with bifurcated fibers, with an average length of 2309 μm. Axial parenchyma was visible only under a 10× magnification lens, diffuse paratracheal, and occurred diffusely in the aggregate; the presence of crystals in parenchyma cells was observed (Fig 7[d] and [e]). Rays are visible to the naked eye in the cross-section and visible only under a 10× lens in the tangential and nonstratified section, with an average height of 674 μm and an average width of 20 μm, constituted by the body of the procumbent cells mainly with 2-4 rows of marginal cells square and/or upright (Fig 7[g]). In macroscopic observation, the mirroring of the rays was considered contrasted in the radial section.

The growth layers demarcated by fibrous zones and the presence of pores obstructed by tylose were also observed by Lopes et al (2019), who analyzed the potential of different wood species used in the manufacturing of artisanal boats in the state of Pará. Braga Júnior et al (2020) also observed the presence of crystals in parenchyma cells in *Caryocar villosum* when assessing the properties of wood used for the production of boats.

Figure 8 shows the anatomical measurements of *Protium altissimum*, and Table 5 shows the summary of the anatomical features. Different growth layers are individualized either by a layer of fibrous tissue (Fig 9[a]) or by bands of parenchyma simulating marginal parenchyma. Pores/vessels were visible only under 10× magnification, diffuse, radial arrangement, mean length 333 μm and mean width 132 μm, 76% solitary, 11% multiples of 2, 7% multiples of 3, 3% multiples of 4, and 2% multiples of >4, with angular contour, obstructed by substance with a shiny appearance on macroscopic view and by tylosis on microscopic view, with simple perforation plate (Fig 9[b]), alternating intervessel pits, ray pits vascular with distinct borders; similar to intervessels in size and shape, in the radius of the cell, in macroscopic observation. The vascular lines were straight in the tangential section. Libriform and septate fibers (Fig 9[c]), with an average length of 990 μm. Axial parenchyma was visible only under 10× magnification, scanty paratracheal (also occurring unilateral type), with three to four cells per strand of parenchyma. Rays are visible to the naked eye in the cross section and are visible only under a 10× lens in the tangential and nonstratified sections, with a mean height of 266 μm and a mean width of 20 μm constituted with the body of the procumbent cells with a row of square marginal cells and/or upright in macroscopic observation; the mirroring of the rays was considered contrasted in the radial section, with the presence of radial channels in fusiform rays (Fig 9[d]). Calcium oxalate crystals (Fig 9[e]) were observed in square and upright ray cells (Fig 9[f]-[h]). Similar characteristics were observed

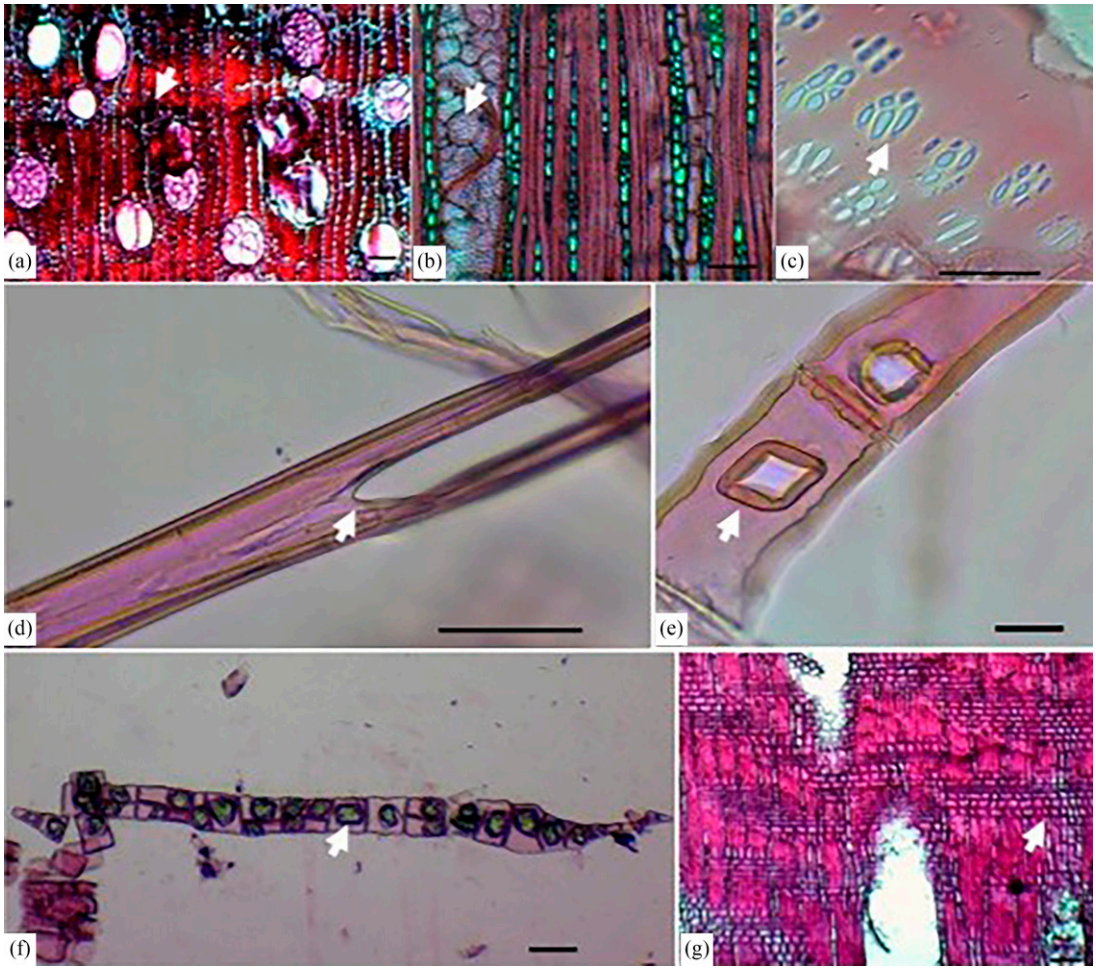

Figure 7. Anatomical features observed *Caryocar villosum*. The arrows on the pictures indicate the following: (a) growth layers and parenchyma similar to marginal, (b) tylosis on vessels from tangential view, (c) horizontal pits horizontal (scalariform, gash-like), (d) bifurcated fibers, (e and f) the presence of prismatic crystals in chambered parenchyma cells, and (g) rays with upright and square marginal cells. Scale bars: (a, e, f, and g) 150 µm, (b) 100 µm, and (c and d) 50 µm.

by Ferreira et al (2021) when studying wood from the Peruvian Amazon forest.

All species presented libriform-type fibers, with a tapered and pointed end, a common characteristic in angiosperm woods (Burger and Richter 1991; Gonçalves et al 2007), in *Astronium lecointei* and *Protium altissimum*, fibers of the type chambered. Metcalfe and Chalk (1983) reported that these may have a substance storage function (as well as parenchyma cells), which may suggest compensation for the low amount of axial parenchyma in these two species, presenting themselves as scarce in *Astronium lecointei* and the scarce and/or unilateral type in *Protium altissimum* (Table 6).

Occasionally, *Jacaranda copaia* and *Caryocar villosum* present bifurcated fibers, these variations are due to intrusive growth, and these may also form intrusive cavities in these cells (Esau 1967; Medeiros et al 2020), not being associated with deterioration as function of the aging time storage.

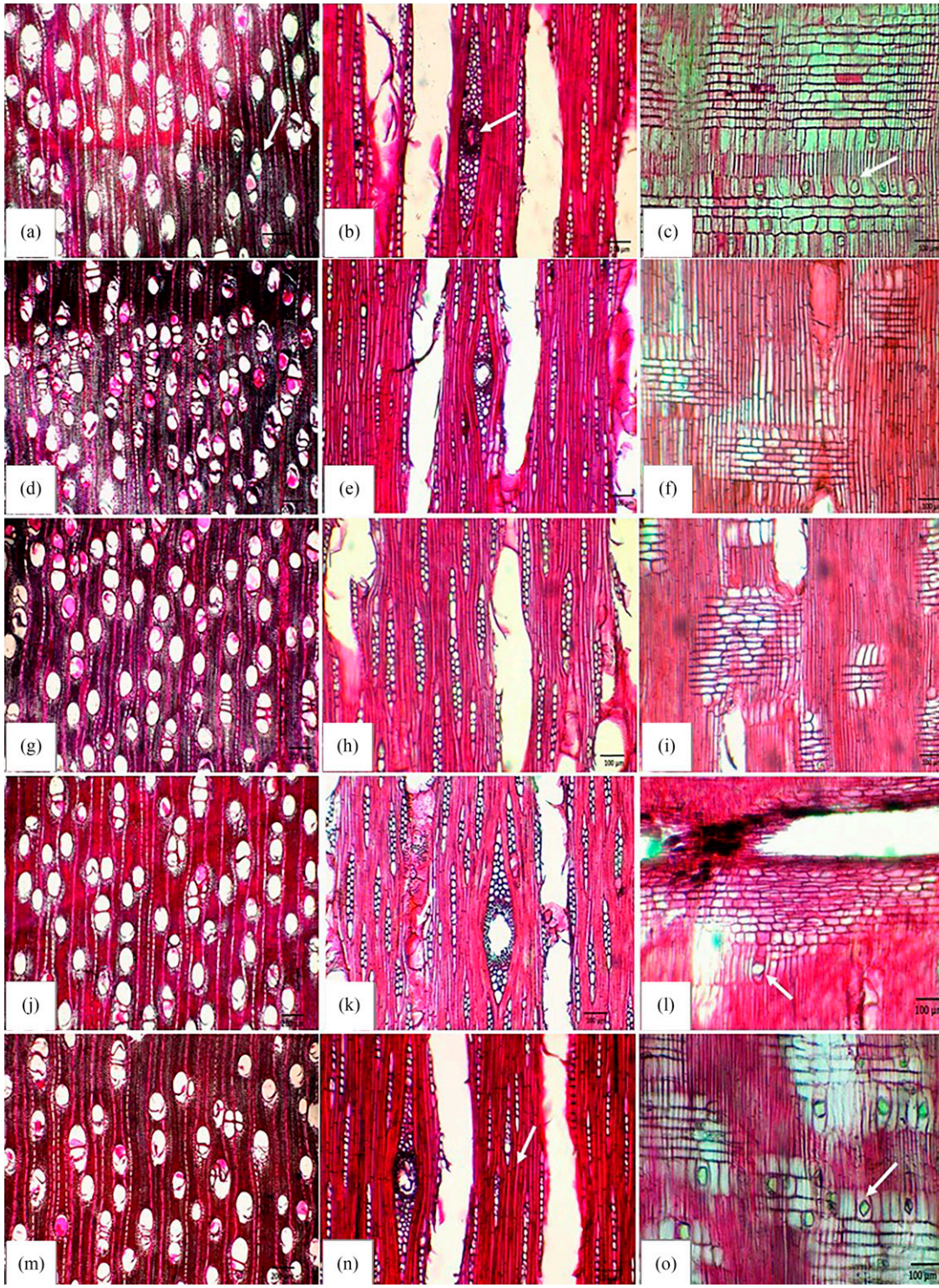

Figure 8. Anatomical elements of *Protium altissimum*. The arrows on the pictures indicate the following: (a-c) With 8 yr of storage, (d-f) with 6 yr of storage, (g-i) with 4 yr of storage, (j-m) with 2 yr of storage, and (n-p) with a period of less than 1 yr of storage. Scale bars: (a, d, g, j, and n) 200 µm and (b, c, e, f, h, i, l, m, o, and p) 100 µm.

Table 5. Anatomical characters of *Protium altissimum* in different storage time (yr).

Anatomical features		Years of exposure					Overall mean
		8	6	4	2	0	
Fibers	Length (μm)	998.7	982.51	964.07	1022.67	986.15	990.82
	Wall thickness (μm)	4	3.94	3.81	4.66	3.31	3.94
	Lumen thickness (μm)	5.47	5.53	5.53	2.92	4.73	4.84
Vessels	Length (μm)	367.51	317.28	326.78	305.65	349.08	333.26
	Diameter (μm)	137.59	130.21	135.74	131.93	127.97	132.69
Rays	Height (μm)	248.03	248.61	203.47	196.94	434.17	266.24
	Width (μm)	20.12	19.06	16.37	18.53	30.14	20.84
	Height (cell counts)	14.62	13.41	13.31	12.6	13.49	13.49
	Width (cell counts)	1.83	1.55	1.56	1.62	1.65	1.64
	Frequency (mm^{-1})	7.26	7.79	7.79	7.45	8.51	7.76

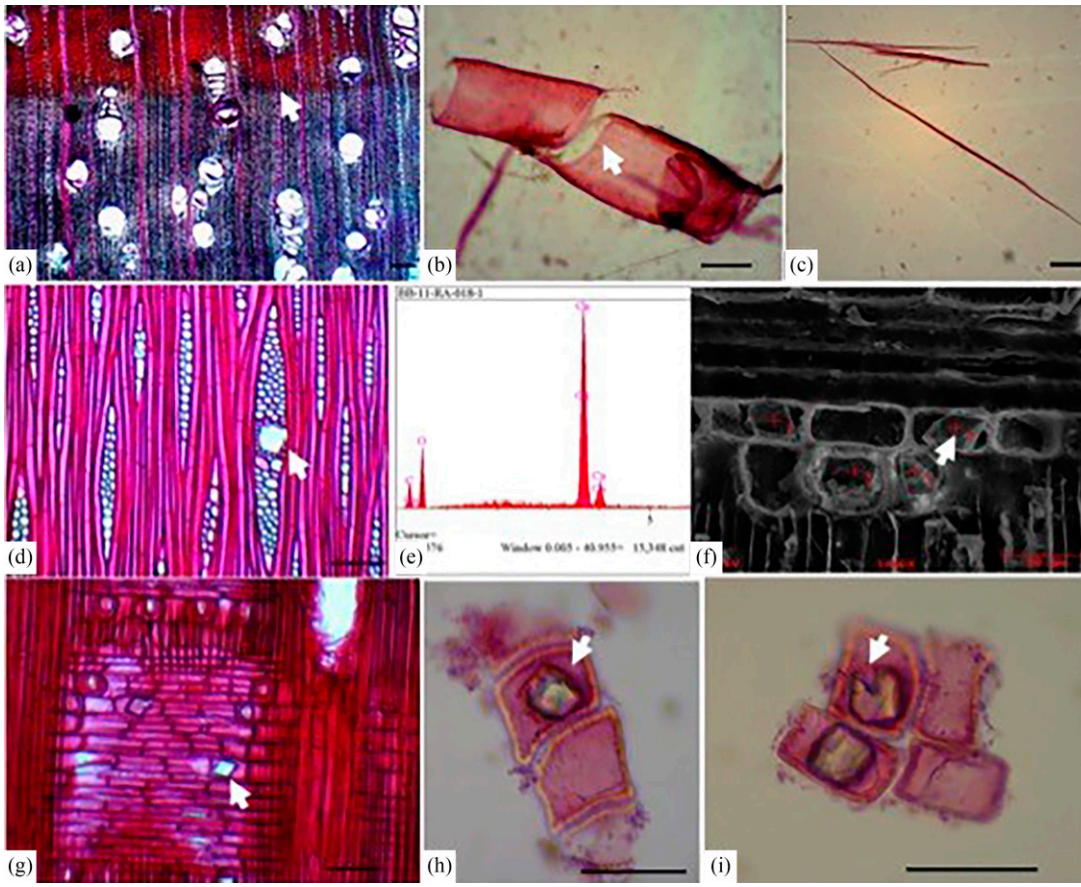

Figure 9. Anatomical features observed *Protium altissimum*. The arrows on the pictures indicate the following: (a) growth layers on cross-section view, (b) simple perforation plates in vessels, (c) libriform fibers, (d) fusiform ray, (e) energy dispersion X-ray spectroscopy confirming the presence of crystals composed of calcium oxalate, and (f, g, h, and i) calcium oxalate crystals in upright and square ray cells. Scale bars: (a and c) 150 μm, (b, d, and g) 100 μm, and (h and i) 50 μm.

Table 6. Polynomial regression equations for length, wall thickness, and lumen thickness of fibers in the analyzed species as a function of storage time (yr).

Variable	Species	Equation	R^2	p
Length (μm)	*Protium altissimum*	$y = 999.02 - 5.95x + 0.65x^2$ (NS)	0.06	0.804
	Caryocar villosum	$y = 2415.98 - 26.69x$ (NS)	0.46	0.229
	Astronium lecointei	$y = 869.76 + 186.94x - 19.91x^2$ (NS)	0.86	0.084
	Jacaranda copaia	$y = 943.23 + 88.15x$ (NS)	0.83	0.200
Wall thickness (μm)	*Protium altissimum*	$y = 3.59 + 0.26x - 0.03x^2$ (NS)	0.24	0.231
	Caryocar villosum	$y = 9.26 - 0.13x$ (NS)	0.48	0.188
	Astronium lecointei	$y = 3.56 + 0.786x - 0.096x^2$ (NS)	0.95	0.093
	Jacaranda copaia	$y = 2.25 + 0.13x$ (NS)	0.89	0.083
Lumen thickness (μm)	*Protium altissimum*	$y = 4.02 + 0.20x$ (**)	0.33	0.010
	Caryocar villosum	$y = 1.99 + 0.14x$ (NS)	0.62	0.258
	Astronium lecointei	$y = 5.23 + 0.37x$ (NS)	0.62	0.128
	Jacaranda copaia	$y = 17.69 + 4.04x - 0.82x^2$ (NS)	1.00	0.403

NS, not significant.

**Significant at 1% probability.

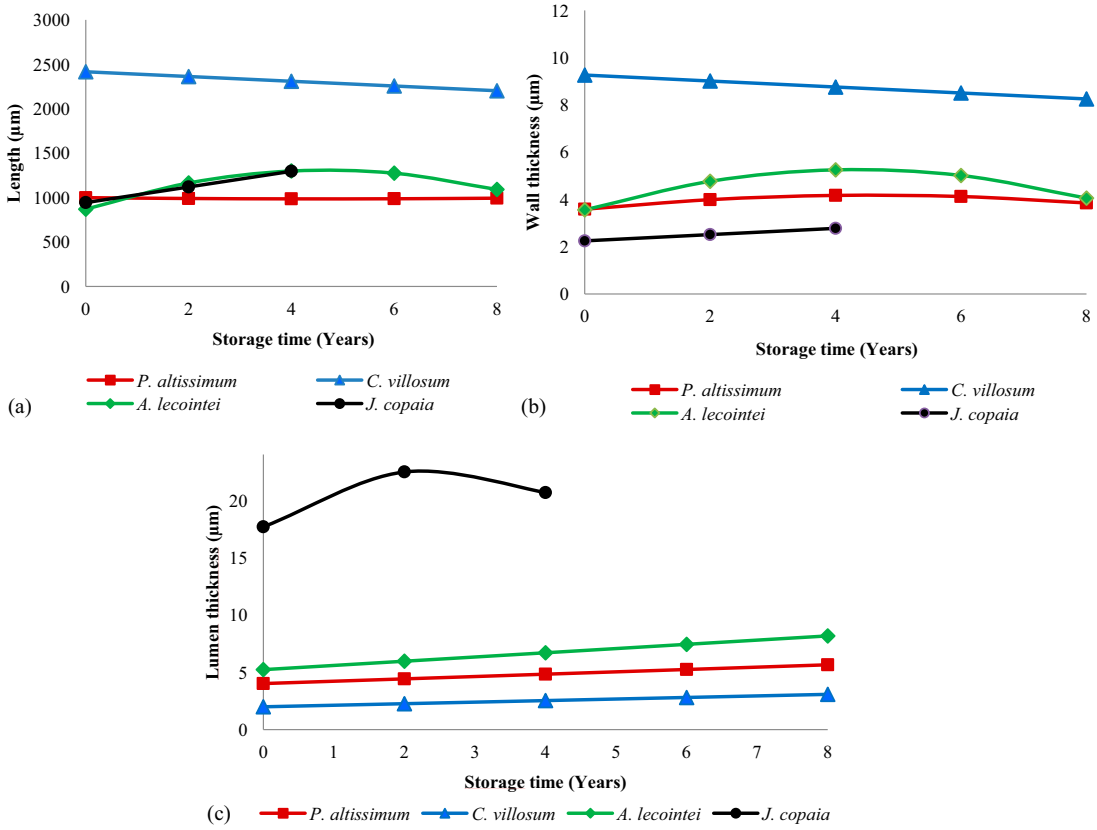

Figure 10. Estimated values of fiber length (a), wall thickness (b), and lumen thickness (c) using polynomial regression equations as a function of storage time (yr), by species.

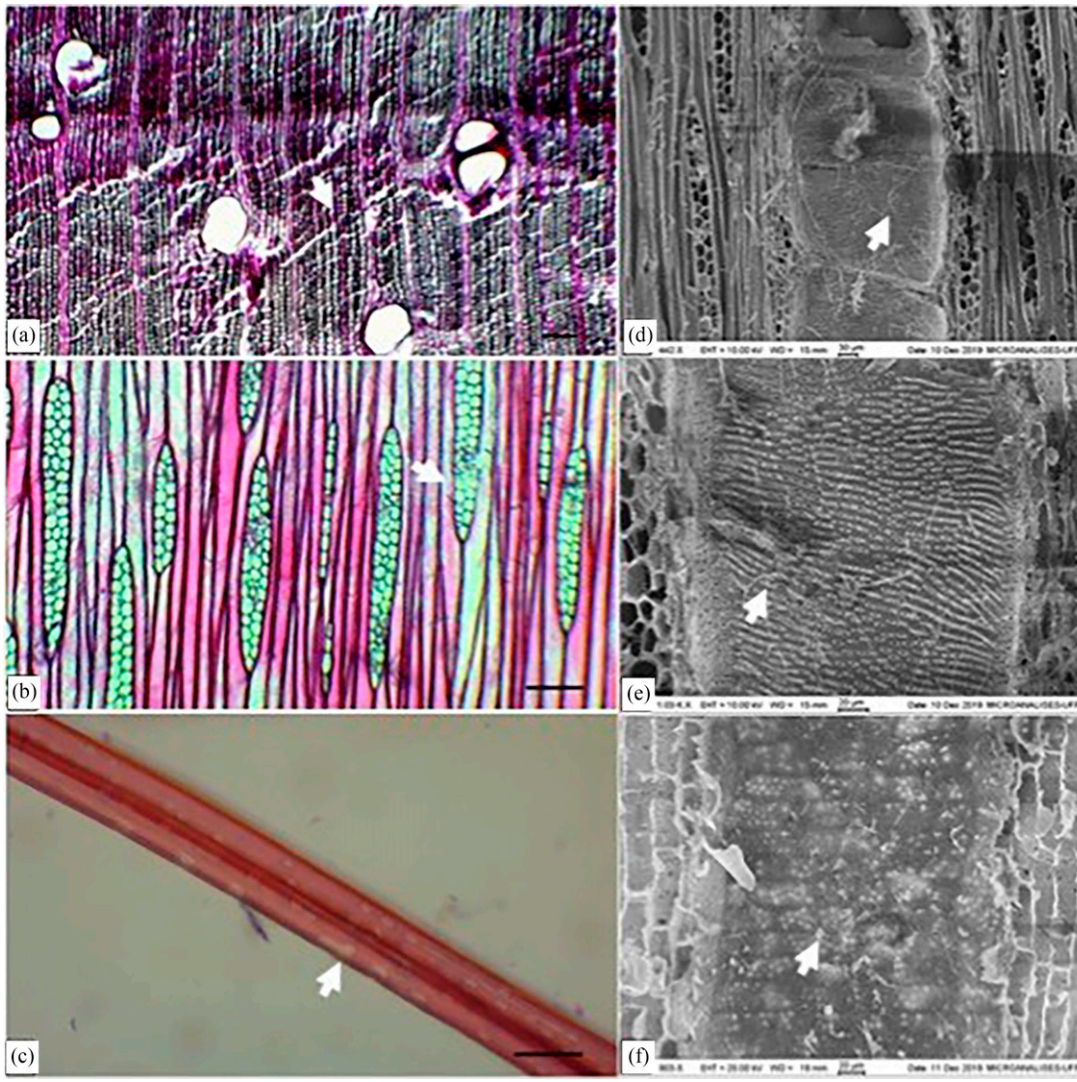

Figure 11. *Jacaranda copaia*. The arrows on the pictures indicate the following: (a) cracks in fibers on samples storage, (b) signs of deterioration on tangential view, (c) fibers in the macerated material showing signs of deterioration by fungi, and (d-f) the presence of hyphae in vessels from scanning electron microscopy images. Scale bars: (a) 150 µm, (b) 100 µm, and (c) 30 µm.

Prismatic calcium oxalate crystals were observed in axial parenchyma cells of *Caryocar villosum*, in radial parenchyma cells of *Protium altissimum,* and both in *Astronium lecointei*. The presence of crystals is frequent in angiosperm wood and can be used as a taxonomic criterion in plant species, as well as in the analysis of difficulties encountered in wood processing (Vasconcelos et al 1995; Costa et al 2006). These mineral inclusions were previously cited in the literature by Nisgoski et al (2012) and Braga Júnior et al (2020) for *Caryocar villosum*, by Albuquerque (2012) for *Astronium lecointei*, and by Ishiguri et al (2003) for *Protium altissimum*.

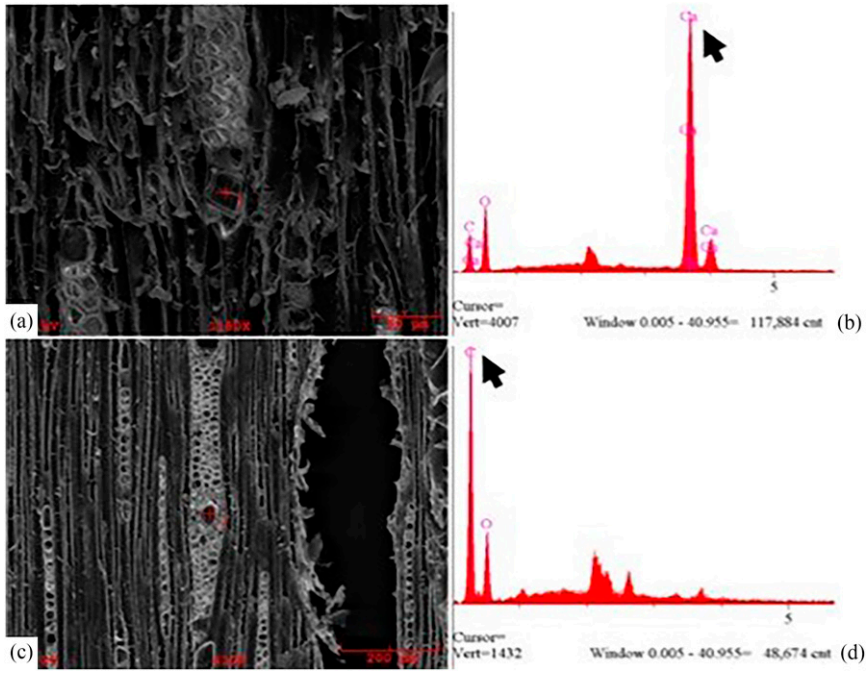

Figure 12. *Astronium lecointei*. The arrows on the pictures indicate the following: (a) the presence of calcium oxalate crystals in rays cells on samples stored for 4 yr, (b) confirmed by energy dispersion X-ray spectroscopy (EDS) analysis; (c) the presence of the carbon content in fusiform ray, and (d) confirmed by EDS analysis.

Caryocar villosum presented the highest fiber length and wall thickness values, followed by *Astronium lecointei*, *Jacaranda copaia* (in length), and *Protium altissimum*. The highest values for lumen thickness were observed in *Jacaranda copaia*, followed by *Astronium lecointei*, *Protium altissimum*, and *Caryocar villosum* (Fig 10). The thickness of the lumen is related to

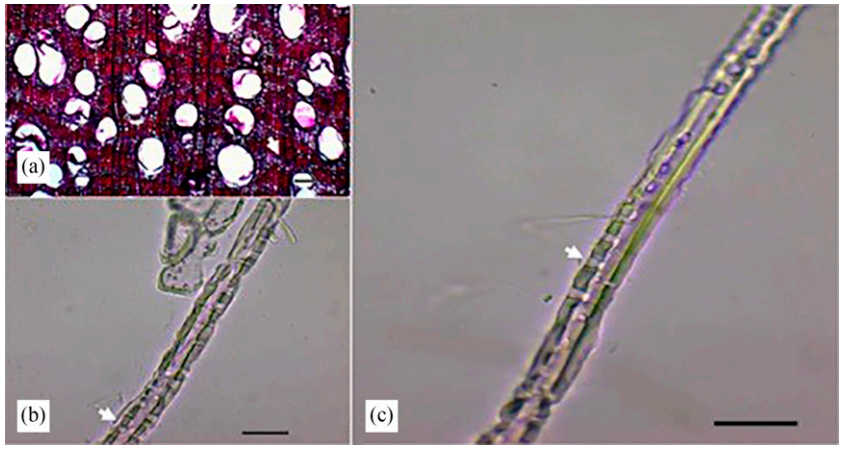

Figure 13. *Caryocar villosum*. The arrows on the pictures indicate the following: (a) A cross-section view showing apotracheal diffuse parenchyma in samples stored for 8 yr, (b) cracks and ruptures on fibers, and (c) discontinued cell wall in fibers. Scale bars: (a) 150 µm and (b and c) 30 µm.

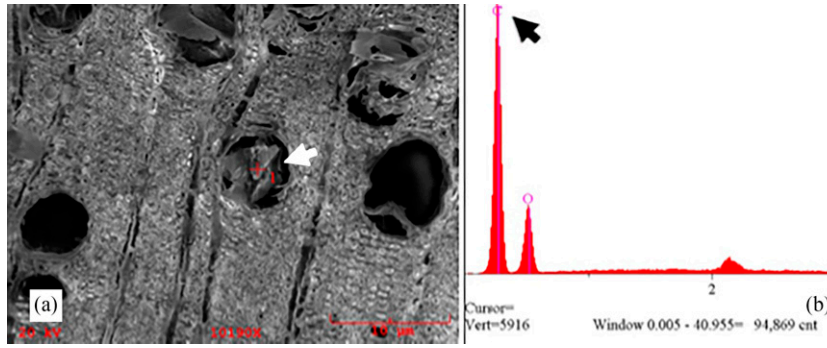

Figure 14. *Protium altissimum.* The arrows in the pictures indicate the following: (a) obstructed vessels by the carbon content in samples stored for 8 yr; and (b) confirmed by energy dispersion X-ray spectroscopy analysis were observed in samples stored for 8 yr.

the thickness of the fiber wall (Oliveira 2003; Belini et al 2008). Thus, the higher the values in the lumen thickness, the emptier spaces will be found in the wood, indicating a lower density.

In general, the variations found in the anatomical structures are influenced by the age of the vascular cambium (Tsoumis 1968), which may be directly related to the age of the plant, as well as the diameter of the logs that were collected.

Overall, samples of *Jacaranda copaia* presented an advanced stage of deterioration compared with the other species studied (Fig 11). Cracks in the fiber lumen observed in *Jacaranda copaia* only occurred in samples stored for 2 and 4 yr. In the SEM analysis, the presence of hyphae in samples was stored for 2 and <1 yr. This characteristic is indicative of fungal decay in samples. The presence of cracks in the cell wall and erosion of the lumen are associated with moderate degrees of brown rot (Wilcox 1968; Blanchette 1991).

In *Astronium lecointei*, no signs of cracks in fibers were observed in all stored times studied. However, the carbon content was noted in vessels of samples with 8 yr of storage, and the presence of calcium oxalate and carbon content was noted in ray cells on samples exposed for 4 yr (Fig 12).

In *Caryocar villosum*, few disruptions in the cell wall of fibers were observed in the samples exposed for 8 yr, which can be an indication of a fungal attack (Fig 13). No fractures were observed in *Protium altissimum*; however, the presence of crystals was noted during the microscopic analysis, and EDS analyses were performed

Table 7. Polynomial regression equations for length and diameter of vessel elements, of the analyzed species as a function of storage time (yr).

Variable	Species	Equation	R^2	p
Length (μm)	*Protium altissimum*	$y = 345.94 - 19.96x + 2.80x^2$ (*)	0.80	0.030
	Caryocar villosum	$y = 598.32 - 7.08x$ (NS)	0.38	0.131
	Astronium lecointei	$y = 328.38 + 2.55x$ (NS)	0.55	0.496
	Jacaranda copaia	$y = 405.17 + 58.06x - 10.06x^2$ (**)	1.00	<0.001
Diameter (μm)	*Protium altissimum*	$y = 129.18 + 0.88x$ (NS)	0.49	0.433
	Caryocar villosum	$y = 243.71 - 7.081x$ (*)	0.94	0.011
	Astronium lecointei	$y = 123.87 + 9.36x - 1.12x^2$ (NS)	0.44	0.186
	Jacaranda copaia	$y = 221.44 + 36.91x - 9.75x^2$ (NS)	1.00	0.131

NS, not significant.
** Significant at 1% probability.
* Significant at 5% probability.

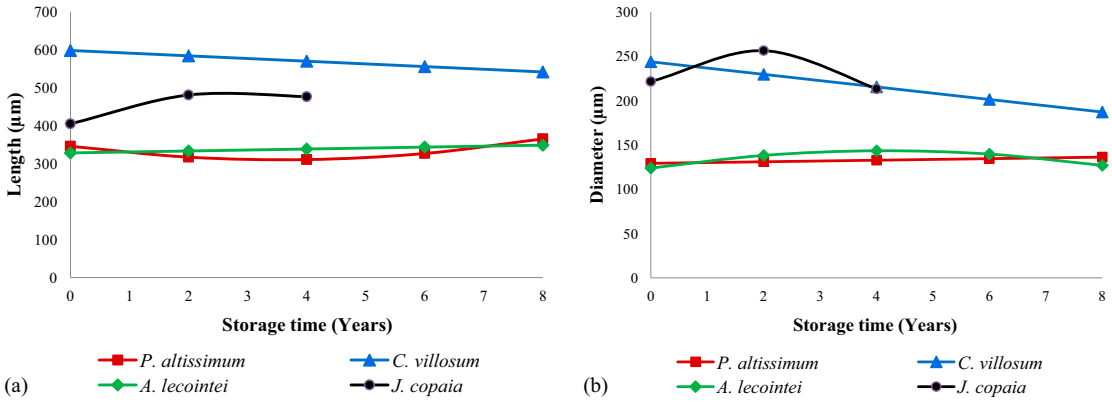

Figure 15. Estimated values of length (a) and diameter (b) of vessel elements using polynomial regression equations as a function of storage time (yr), by species.

and obstructed vessels with the presence of carbon were observed in the samples stored for 8 and 2 yr. The carbon content was also present in rays in samples exposed for 8 yr (Fig 14), which is not common to occur and can also be considered a sign of a fungal attack.

The anatomical variables were submitted to statistical analysis, demonstrating that the polynomial regression models were significant for the vessel element parameter, in terms of length for *Protium altissimum* and *Jacaranda copaia* and in terms of diameter for *Caryocar villosum* (which also

Table 8. Polynomial regression equations for length and width (µm and number of cells) and frequency per linear millimeter in rays, of the analyzed species as a function of storage time (yr).

Variable	Species	Equation	R^2	p
Height (µm)	*Protium altissimum*	$y = 403.50 - 89.16x + 9.14x^2$ (**)	0.77	0007
	Caryocar villosum	$y = 781.58 - 26.80x$ (**)	0.73	<0001
	Astronium lecointei	$y = 329.54 + 16.27x - 2.05x^2$ (NS)	0.79	0279
	Jacaranda copaia	$y = 363.87 - 49.55x + 10.19x^2$ (NS)	1.00	0265
Width (µm)	*Protium altissimum*	$y = 29.06 - 5.29x + 0.54x^2$ (NS)	0.89	0053
	Caryocar villosum	$y = 18.32 + 1.66x - 0.18x^2$ (NS)	0.17	0426
	Astronium lecointei	$y = 23.58 - 1.45x + 0.24x^2$ (NS)	0.67	0079
	Jacaranda copaia	$y = 35.46 - 0.60x - 0.02x^2$ (NS)	1.00	0990
Height (number of cells)	*Protium altissimum*	$y = 13.39 - 0.36x + 0.06x^2$ (NS)	0.89	0302
	Caryocar villosum	$y = 26.88 - 1.30x + 0.14x^2$ (NS)	0.23	0161
	Astronium lecointei	$y = 17.13 - 0.23x$ (NS)	0.78	0426
	Jacaranda copaia	$y = 16.05 - 1.44x + 0.34x^2$ (NS)	1.00	0282
Width (number of cells)	*Protium altissimum*	$y = 1.68 - 0.08x + 0.01x^2$ (NS)	0.80	0304
	Caryocar villosum	$y = 1.57 + 0.03x$ (NS)	0.78	0157
	Astronium lecointei	$y = 2.05 - 0.16x + 0.03x^2$ (NS)	0.36	0126
	Jacaranda copaia	$y = 2.50 - 0.10x$ (NS)	0.67	0251
Linear frequency (mm)	*Protium altissimum*	$y = 8.19 - 0.11x$ (NS)	0.52	0183
	Caryocar villosum	$y = 9.94 + 0.52x - 0.05x^2$ (NS)	0.98	0331
	Astronium lecointei	$y = 6.85 - 0.19x + 0.02x^2$ (NS)	0.21	0713
	Jacaranda copaia	$y = 4.97 - 0.15x$ (NS)	0.96	0198

NS, not significant.
** Significant at 1% probability.

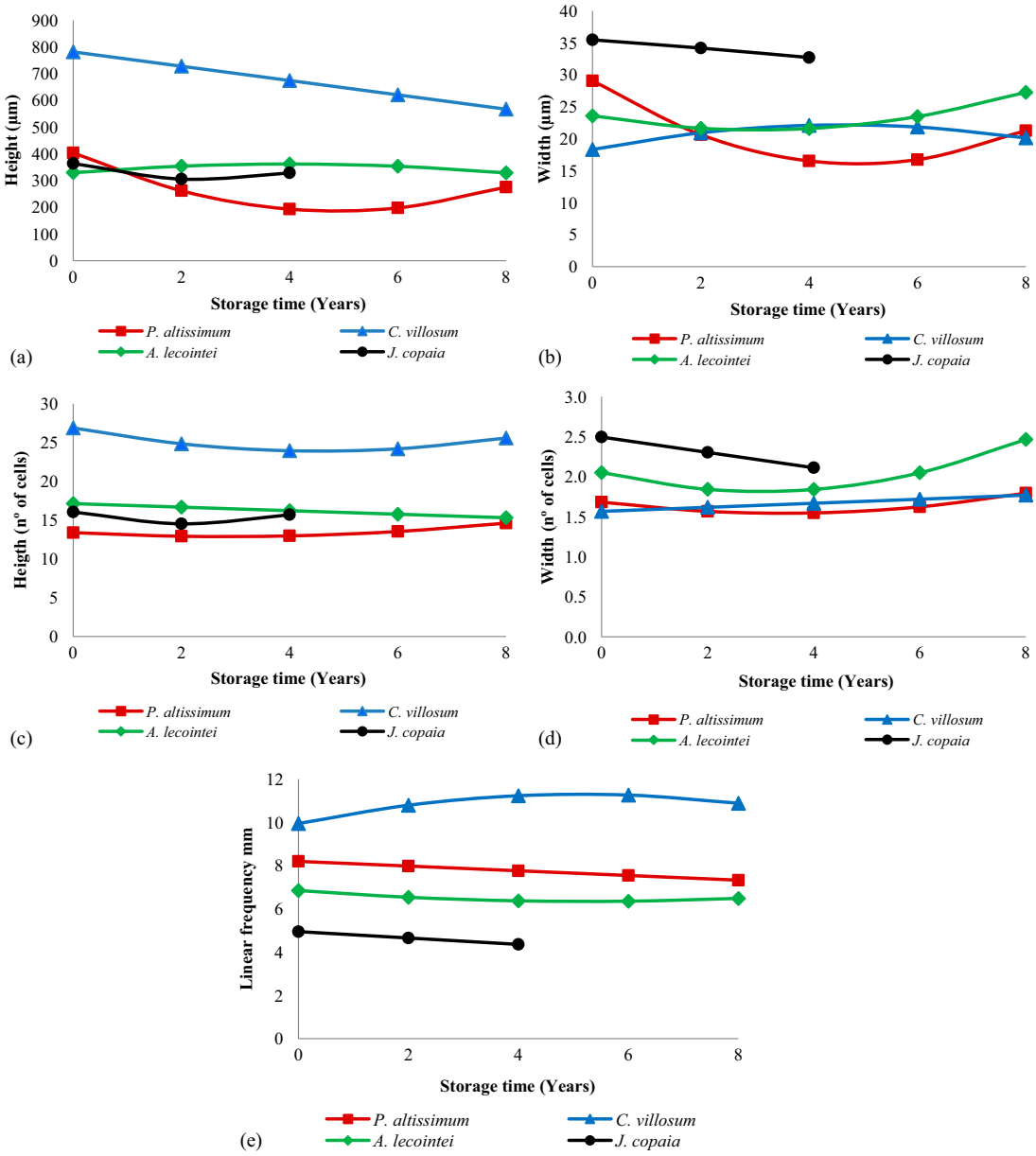

Figure 16. Estimated values of height (a) and width (b) in micrometers (µm) and height (c) and width (d) in the number of cells and frequency per linear millimeter (e) of the rays, through the equations of polynomial regression as a function of storage time.

presented the highest value in length), followed by *Jacaranda copaia*, indicating that the storage time has no effect on the dimensions of this cellular element in the other species.

The quantitative parameters of wood anatomy may vary between individuals and even within the individual, depending on the trunk's height and the position in which the samples were taken

(Ishiguri et al 2003). *Caryocar villosum* and *Jacaranda copaia* presented vessel elements with a diameter greater than 200 µm, and Wheeler and Baas (1991) mentioned that this is a frequent value in tropical species.

Astronium lecointei, *Caryocar villosum*, and *Protium altissimum* occasionally presented tylosis in the vessel elements. According to Zimmermann (1978), tylosis can be related to protrusions of parenchyma cells close to the vessel element that penetrate the lumen of conducting vessels through your scores.

Narrower vessels with thicker walls are generally associated with high-density woods (Anselmo 2015); however, this was not observed in the present study, since the four species studied were considered of medium density (except for *Jacaranda copaia* – considered of low density), presenting large vessel elements, with a diameter greater than 100 µm.

Table 7 shows the trends for vessel elements analyzed in the four species studied in different exposure times, and values expressed graphically are shown in Fig 15. In the fibers, the polynomial regression analyses were considered significant in terms of lumen thickness for *Protium altissimum*, suggesting that the storage time did not affect the length, width, and thickness of the lumen of the other species studied.

In the rays, the polynomial regression analyses were considered significant in terms of height (µm) for *Protium altissimum* (Table 8) indicating that there was no influence of storage time in the ray in height and width (number of cells and µm) and frequency per linear millimeter (Fig 16).

In the ascending order, wider rays were observed in *Jacaranda copaia*, *Protium altissimum*, *Astronium lecointei*, and *Caryocar villosum*, which is associated with the storage function and lateral translocation of solutes at short distances (Costa et al 2006).

In general, wood species with more abundant radial parenchyma (such as *Jacaranda copaia*) tend to be more susceptible to fungal attack. Silva and Aguiar (2001) analyzed the degradation of the wood of *Hura creptans* by lignolytic fungi belonging to the *Hymenomycetes* class and observed that after the colonization of the vessel elements, penetrating the wall through the pits, the fungi quickly colonized the ray cells, resulting in an advanced stage of degradation.

CONCLUSIONS

This study described the anatomical features of four commonly used wood species (*Jacaranda copaia*, *Astronium lecointei*, *Caryocar villosum*, and *Protium altissimum*) from the Amazon forest in Brazil and provided anatomical characterization of wasted logs during mining activity on different time ranges. The results of this study increase the knowledge base on anatomical features of tropical species from the Amazon forest and provide baseline information to identify potential end uses for the logs that are left in open storage in other mining areas, consequently allowing for better utilization of natural resources while minimizing economic and environmental impacts.

It was possible to distinguish and characterize the species based on anatomy, and the primary diagnostic features for the identification of species were vessels, rays, parenchyma, and fibers. As expected, anatomical features did not change over time, but the changes observed in the wood anatomy enable us to identify the presence of the fungal degradation process in the species studied.

Among all four species studied, *Jacaranda copaia* showed advanced stages of fungal degradation, presenting cracks in fibers on samples exposed for 2 and 4 yr. In addition, the presence of hyphae was observed in samples exposed for less than 1 yr. In *Astronium lecointei*, no signs of cracks were observed in all samples. However, the carbon content was present in vessel elements of samples exposed for 8 yr and was present in ray cells in samples exposed for 4 yr. In *Caryocar villosum*, few disruptions in fiber cells were found on samples exposed for 8 yr, and the carbon content was also observed in *Protium altissimum* exposed for 8 yr.

REFERENCES

Albuês TAS, Maria DMB, Madi JPS, Caldeira SF, Silva KDT (2023) Degree of infestation and preferences of hemiparasites in urban arborization. Rev Arvore 47:e4707.

Albuquerque AR (2012) Comparative anatomy of the wood and charcoal applied in the identification of 75 species of the Amazon forest in the state of Pará, Brazil. MS thesis, Escola Superior de Agricultura "Luiz de Queiroz", Piracicaba, Brazil, 250 pp (In Portuguese with English abstract).

ANAGNOST SE (1998) Light microscopic diagnosis of wood decay. IAWA Journal 19(2):141-67.

Anselmo GC (2015) Relations between anatomical characters of xylem, wood density and hydraulic safety in semiarid species. MS thesis, Universidade Federal do Ceará, Fortaleza. 49 pp (In Portuguese with English abstract).

Arantes V, Milagres AMF (2009) Relevance of low molecular weight compounds produced by fungi and involved in wood biodegradation. Fortaleza, Quim Nova 32(6):1586-1595 (In Portuguese with English abstract).

Barbosa AP, Campos MAA, Sampaio PTB, Nakamura S, Gonçalves CQB (2003) Growth of two forest pioneer species, pau-de-balsa (*Ochroma lagopus* Sw.) e caroba (*Jacaranda copaia* D. Don), used for rehabilitation of degraded areas from agriculture in Central Amazon, Brazil. Acta Amazon 33(3):477-482 (In Portuguese with English abstract).

Barbosa JC, Maldonado JW (2015) Agrostat–software for statistical analysis for agronomic experiments. Version 1.1. 0.711. Funep, Jaboticabal, Brazil.

Belini UL, Tomazello M, Chagas MP, Dias CTS (2008) Characterization of wood anatomy, basic density, and morphology of *Eucalyptus grandis* chips for MDF production. FLORAM 32(4):707-713 (In Portuguese with English abstract).

Blanchette RA (1991) Delignification by wood-decay fungi. Ann Rev Phytopathol 29:381-398.

Braga DPP, Ruschel AR, Kanashiro M, Vidal E, Cruz ED, Miléo RC, Porro R (2021) Trees from forest management in the Virola Jatobá Sustainable Development Project Anapu, PA. Embrapa, Brasília, Brazil. 196 pp (In Portuguese).

Braga Júnior MM, Matos TS, Andrade GM, Ferreira PS, Silva MCF, Souza FIB, Melo LEL (2020) Technological properties of woods used in boat's production in the Southeast of Pará, Brazil. Rodriguésia 71:e03322018.

Burger LM, Richter HG (1991) Anatomy of wood. Nobel, São Paulo, Brazil. 154 pp (In Portuguese).

Cahuana LAP, Guevara BAH, Luque EMM, Palermo GPM, Latorraca JVF (2021) Dendrochronology of two forest species in the urban area of the city of Puerto Maldonado, Peru. Floresta 51(3):703-712.

Cerqueira RM, Jardim MAG, Silva Junior LLM, Paixão LP, Martins MB (2021) Phytosociology of the tree level in native forest areas and in degraded areas recovery program under the influence of mining, Paragominas, Pará, Brasil. Nat Conserv 14(3):22-41 (In Portuguese with English abstract).

Coradin VTR, Muñiz GIB (1992) Standard for wood anatomy in: Angiospermae e Gymnospermae. Laboratório de Produtos Florestais. Ser Tec 15:1-19 (Brasília).

Costa CG, Callado CH, Coradin VTR, Carmelo-Guerreiro SM (2006) Xylem. Pages 129-154 *in* B Appezzato-da-Glória and SM CarmelloGuerreiro, eds. Plant anatomy, 2nd edition. Editora UFV, Viçosa, Brazil (In Portuguese).

Costa JA (2017) Classification of Amazonian woods for the composition of string musical instruments using the impulse excitation technique. MS thesis, Universidade Federal do Amazonas, Manaus, Brazil. 127 pp (In Portuguese with English abstract).

Duarte PJ, Borges CC, Ferreira CA, Cruz TM, de Souza WRQ, Mori FA (2021) Anatomical identification of tropical woods traded in Lavras, Brazil. J Trop For Sci 33(1):95-103.

Dudka S, Adriano DC (1997) Environmental impacts of metal ore mining and processing: A review. J Environ Qual 26:590-602.

Esau K (1967) Plant anatomy, 2nd edition. John Wiley & Sons, New York, NY. 768 pp.

Farias-Singer R (2020) Jacaranda in Flora of Brasil 2020. Jardim Botânico do Rio de Janeiro.

Ferreira CA, Inga JG, Vidal OD, Goytendia WE, Moya SM, Centeno TB, Vélez A, Gamarra D, Tomazello-Filho M (2021) Identification of tree species from the Peruvian Tropical Amazon "Selva Central" forests according to wood anatomy. BioResources 16(4):7161-7179.

Franklin GL (1945) Preparation of thin sections of synthetic resins and woody resin composites and a new method for wood. Nature 155:3924-3951.

Gomes JI, Ferreira GC, Urbinati C (2002) Anatomy and identification of Amazonian woods. Embrapa Amazônia Oriental, Belém, Brazil (In Portuguese).

Gomes VHF, Vieira ICG, Salomão RP, Steege H (2019) Amazonian tree species threatened by deforestation and climate change. Nat Clim Chang 9(7):547-553.

Gonçalves MPM, Ranusa C, Carvalho AM, Apda GR (2007) Radial variation of basic density and fiber length of the wood of *Tectona grandis* L. FLORAM 14(1):70-75 (In Portuguese with English abstract).

Gonçalves TAP, Scheel-Ybert R (2016) Charcoal anatomy of Brazilian species. I. Anacardiaceae. An Acad Bras Cienc 88:1711-1725.

IAWA Committee (1989) List of microscope features for hardwood identification. IAWA Bull New Ser 10(3): 234-332.

Ishiguri F, Maruyama S, Takahashi K, Abe Z, Yokota S, Andoh M, Yoshizawa M (2003) Extractives relating to heartwood color changes in sugi (*Cryptomeria japonica*) by a combination of smoke-heating and UV radiation exposure. J Wood Sci 2003(49):135-139.

Johansen DA (1940) Plant microtechnique. McGraw-Hill, New York, NY. 523 pp.

Kuresk R, Moreira VR, Veiga CP (2020) Agribusiness participation in the economic structure of a Brazilian

region: Analysis of GDP and indirect taxes. Rev Econ Sociol Rural 58(3):e207669.

Lopes OP, Carvalho AG, Zanuncio AJV, Alves MM, Macedo EG (2019) Wood species used in craft boats in Pará state – Brazil 1. Rev Inst Flor 31(2):119-129.

Machado MR, Camara R, Sampaio PTB, Pereira MG, Ferraz JBS (2017) Land cover changes affect soil chemical attributes in the Brazilian Amazon. Acta Sci Agron 39(3):385-391.

Mahar D (1988) Government policies and deforestation in Brazil's Amazon region. World Bank, Washington, D.C.

Medeiros SM, Sousa LKVS, Ferreira CI, Vieira G, Tomazello M (2020) Comparative anatomy of oleoresin producing and non-producing trees of *Copaifera multijuga* Hayne in primary forests and plantations. Flora 263:1-13.

Melo LEL, Silva CJ, Urbinatti CV, Santos IS, Soares WF (2013) Anatomical variation in the wood of *Astrnium lecointei* Ducke. Floresta Ambient 20(1):135-142.

Metcalfe CR, Chalk L (1983). Anatomy of the dicotyledons: Volume 2: Wood structure and conclusion of the general introduction, 2nd edition. Oxford University Press, Cary, NC. 297 pp.

Nisgoski S, Muñiz GIB, França RF, Batista FRR (2012) *Copaifera* cf. *langsdorfii* Desf. and *Dipteryx odorata* (Aubl.) Wild. charcoal anatomy. Braz J Wood Sci 3(2): 66-79.

Oliveira E (2003) Chemical, anatomic and thermal characteristics of the wood of three species with great occurrence in the Northeastern (Brazilian) semi-arid. Dissertation, Universidade Federal de Viçosa, Viçosa, Brazil. 149 pp (In Portuguese with English abstract).

Pace MR, Lohmann LG, Olmstead RG, Angyalossy V (2015) Wood anatomy of major Bignoniaceae clades. Plant Syst Evol 301:967-995.

Parrotta JA, Knowles OH (2002) Restoration of tropical moist forests on bauxite-mined lands in the Brazilian Amazon. Restor Ecol 7(2):103-116.

Paula JE (1977) Anatomy of Amazon woods for production of pulp and paper. Acta Amazon 7(2):273-288 (In Portuguese).

Pimentel EN (2009) General aspects of the Paragominas bauxite mine comparative study and development of optimal operational logistics models – shift change. Final Paper, Universidade Fereal do Pará, Belém, Brazil. 51 pp (In Portuguese with English abstract).

Piva LRO, Sanquetta CR, Wojciechowski J, Corte APD (2020) Phytosociology in forest communities of Radambrasil project in the Amazon biome. Biofix Sci J 5(2): 264-271 (In Portuguese with English abstract).

Prance GT, Pirani JR (2023) Caryocaraceae in Flora e Funga do Brasil. Jardim Botânico do Rio de Janeiro. https://floradobrasil.jbrj.gov.br/FB16721 (2 May 2023) (In Portuguese).

Ripley EA, Redmann RE (1996) Environmental effects of mining, 1st edition. St. Lucie Press, Delray Beach, FL.

Rodrigues RA (2023). Glued laminated timber structural elements made with *Jacaranda copaia* wood and externally reinforced with native Amazonian woods through *Ricinus vulgaris* based polyurethane. MS thesis, Escola Superior de Agricultura "Luiz de Queiroz", Piracicaba, Brazil. 59 pp (In Portuguese with English abstract).

Santos G, Miller RB (1997) Wood anatomy of Jacaranda (Bignoniaceae): Systematic relationships in sections monolobus and dilobos as suggested by twig and stem wood rays. IAWA J 18:369-383.

Sgai RD (2000) Factors that affect treating of wood. MS thesis, Universidade Estadual de Campinas, Campinas, Brazil. 130 pp (In Portuguese).

Silva AC, Aguiar IJA (2001) Micromorphology of wood degradation of Amazonian species *Hura crepitans* L. by ligninolytic fungi belonging to Hymenomycetes class. Acta Amazon 31(3):397-418 (In Portuguese with English abstract).

Silva APM, Viana JP, Cavalcante ALB (2012) Diagnosis of solid waste of the mining activity of non-energetic substances. Relatório de pesquisa, IPEA, Brasília, Brazil. 46 pp (In Portuguese).

Silva-Luz CL, Pirani JR, Pell SK, Mitchell JD (2023) *Anacardiaceae* in flora and fungal of Brazil. Jardim Botânico do Rio de Janeiro. https://floradobrasil.jbrj.gov.br/FB15466 (2 May 2023) (In Portuguese).

Silveira MF, Oliveira JRV, Silva ASVS, Gouveia FN (2021) Natural durability of Amazonian wood, 1st edition. Ministério da Agricultura Pecuária e Abastecimento/ Serviço Florestal Brasileiro (MAPA/AECS), Brasília, Brazil. 24 pp (In Portuguese).

Soares WF, Melo LEL, Lisboa PLB (2013) Anatomy of five wood species marketed as 'Sucupira'. Floresta Ambient 21(1):114-125 (In Portuguese with English abstract).

Spletozer AG, Rodrigues L, Santos CR, Koch AK, Zanuncio JC, Soares-Lopes CRA (2023) Composition and structure of tree species in two forest fragments in southern Amazon region. Braz J Bot 46:189-203.

Tsoumis G (1968) Wood as raw material. Pergamon Press, Oxford, UK. 276 pp.

Vasconcelos FJ, Freitas JA, Silva AC (1995) Microscopical observation of mineral inclusions in xylem of tropical wood. Acta Amazon 25(1-2):55-68 (In Portuguese with English abstract).

Wheeler EA, Baas PA (1991) Survey of the fossil record for dicotyledonous wood and its significance for evolutionary and ecological wood anatomy. IAWA Bull 12: 275-332.

Wilcox WW (1968) Changes in wood microstructure through progressive stages of decay. US For. Servo Res. Pap. FPL-70. 46 pp.

Wilcox WW (1970) Anatomical changes in wood cell walls attacked by fungi and bacteria. Bot Rev 36:1-28.

Zabel RA, Morrell JJ (2020) Wood Microbiology. Academic Press, San Diego, CA. 556 pp.

Zimmermann MH (1978) Vessel ends and the disruption of water flow in plants. Phytopathology 68:253-256.